Physics Scholarship   Physics

7-1-2009

Near-infrared photoabsorption by C(60) dianions in a storage ring

U. Kadhane

J. U. Andersen

E. Bonderup

B. Concina

P. Hvelplund

See next page for additional authors

Authors

U. Kadhane, J. U. Andersen, E. Bonderup, B. Concina, P. Hvelplund, M. Kirketerp, B. Suhr, B. Liu, S. Bronsted Nielsen, S. Panja, J. Rangama, K. Stochkel, and S. Tomita

Near-infrared photoabsorption by C60 dianions in a storage ring

U. Kadhane, J. U. Andersen, E. Bonderup, B. Concina, P. Hvelplund et al.

Additional information on J. Chem. Phys.

Near-infrared photoabsorption by C$_{60}$ dianions in a storage ring

U. Kadhane,[1,a)] J. U. Andersen,[1,b)] E. Bonderup,[1] B. Concina,[1] P. Hvelplund,[1]
M.-B. Suhr Kirketerp,[1] B. Liu,[1] S. Brøndsted Nielsen,[1] S. Panja,[1] J. Rangama,[1]
K. Støchkel,[1] S. Tomita,[1] H. Zettergren,[1] K. Hansen,[2] A. E. K. Sundén,[2] S. E. Canton,[3]
O. Echt,[4] and J. S. Forster[5]

[1]*Department of Physics and Astronomy, Aarhus University, DK-8000 Aarhus C, Denmark*
[2]*Department of Physics, University of Gothenburg, SE-41296 Göteborg, Sweden*
[3]*Department of Chemical Physics, Lund University, SE-22100 Lund, Sweden*
[4]*Department of Physics, University of New Hampshire, Durham, New Hampshire 03824, USA*
[5]*Department of Physics, University of Montreal, H3C 3J7 Quebec, Canada*

We present a detailed study of the electronic structure and the stability of C$_{60}$ dianions in the gas phase. Monoanions were extracted from a plasma source and converted to dianions by electron transfer in a Na vapor cell. The dianions were then stored in an electrostatic ring, and their near-infrared absorption spectrum was measured by observation of laser induced electron detachment. From the time dependence of the detachment after photon absorption, we conclude that the reaction has contributions from both direct electron tunneling to the continuum and vibrationally assisted tunneling after internal conversion. This implies that the height of the Coulomb barrier confining the attached electrons is at least ~1.5 eV. For C$_{60}^{2-}$ ions in solution electron spin resonance measurements have indicated a singlet ground state, and from the similarity of the absorption spectra we conclude that also the ground state of isolated C$_{60}^{2-}$ ions is singlet. The observed spectrum corresponds to an electronic transition from a t_{1u} lowest unoccupied molecular orbital (LUMO) of C$_{60}$ to the t_{1g} LUMO+1 level. The electronic levels of the dianion are split due to Jahn–Teller coupling to quadrupole deformations of the molecule, and a main absorption band at 10723 cm^{-1} corresponds to a transition between the Jahn–Teller ground states. Also transitions from pseudorotational states with 200 cm^{-1} and (probably) 420 cm^{-1} excitation are observed. We argue that a very broad absorption band from about 11 500 cm^{-1} to 13 500 cm^{-1} consists of transitions to so-called cone states, which are Jahn–Teller states on a higher potential-energy surface, stabilized by a pseudorotational angular momentum barrier. A previously observed, high-lying absorption band for C$_{60}^{-}$ may also be a transition to a cone state. © *2009 American Institute of Physics*. [DOI: 10.1063/1.3149775]

I. INTRODUCTION

Fullerene anions are of broad interest, e.g., in high-T_c superconductivity[1,2] and molecular electronics.[3,4] In the dianions, the second electron is confined by a Coulomb barrier,[5] and fullerenes are ideal for studies of the dependence of the stability on the size of the dianion.[6] The dominant decay mode is electron tunneling through the Coulomb barrier, analogous to nuclear alpha decay, and the lifetime can be long even for negative binding.

Information on the level structure can be obtained from optical spectroscopy, and C$_{60}^{2-}$ is of special interest because of the competition between Coulomb repulsion between the two electrons and Jahn–Teller (JT) coupling to quadrupole distortions of the highly symmetric C$_{60}$ cage (icosahedral symmetry).[7–9] The interest in this problem has been stimulated by the discovery of superconductivity in alkali ful-

lerides at relatively high temperatures.[1] The electron pairing leading to superconductivity is believed to originate in the JT coupling.[2,10,11]

In accordance with Hund's rules, the Coulomb energy is lowest in the triplet states, but the JT effect is strongest in the singlet state. Measurements on dianions in frozen solution indicate a singlet ground state with a close-lying triplet level,[12,13] but the delicate balance between Coulomb repulsion and JT coupling could be influenced by interactions with the matrix. Gas-phase measurements are needed as a benchmark for theory.

Owing to the weak binding of the second electron it is difficult to produce long lived dianions of C$_{60}$, but we have developed a method for production of intense beams of C$_{60}^{-}$ ions and cold electron attachment to the monoanions in a Na vapor cell.[14] Subsequent storage in an electrostatic ring has allowed detailed studies of the stability of C$_{60}^{2-}$ ions.[15] We concluded that the dianions are metastable in the ground state, with a lifetime of about 20 s (at $T=0$ K) and an energy of about 0.2 eV above that of the monoanion plus a free electron. Results of near-infrared laser spectroscopy on stored dianions are presented here.

II. EXPERIMENTAL DETAILS

The experiments were carried out at the electrostatic storage ring ELISA illustrated in Fig. 1.[16,17] Previously,[15] we used an electrospray source to produce a beam of C_{60}^- ions, but the electrospray is very unstable for fullerene anions. We have therefore constructed a new source based on a plasma source capable of delivering stable nanoampere currents of fullerene anions.[18,19] Hot C_{60}^- ions were extracted from the plasma source and focused by an Einzel lens into a 14-pole linear ion trap with a He trapping gas, which could be cooled to a temperature below 100 K by liquid nitrogen in a container around the trap. The ions were accumulated and stored for 0.1 s and then ejected as a 20–50 μs long bunch. After acceleration to 22 keV and mass selection with a magnet, the ions passed through a cell containing Na vapor, where dianions were formed by electron transfer. These ions were then stored in the ring with revolution time 108.15 μs.

For C_{60} anions in solution or in a solid matrix there are often several charge states present, and it can be difficult to separate their contributions to the absorption. Below we discuss a case where a feature of absorption in the dianion has been ascribed to the monoanion. In our experiment, the ring voltages select a single charge state but the beam could contain dianions of C_{60} isomers. Such a contamination was observed in Ref. 15 as a very small stable component. It is very likely that it consisted of ions with lower symmetry of the C_{60} cage structure (with pairs of adjacent pentagons). As shown in Ref. 20, such molecules have higher electron affinities and therefore should be more stable as dianions. Lifetime measurements with the new ion source have confirmed that the stable component is far too small to give a significant contribution to the absorption spectrum.

The laser used for spectroscopy was an optical parametric oscillator (OPO) pumped with third harmonic radiation from a Nd-doped yttrium-aluminum garnet laser with a pulse energy of about 1 mJ and a pulse length of 3 ns. The intensity profile of the laser is smooth, and the direction of the laser beam varies very little with wavelength, so the overlap with the ion beam could be kept constant in wavelength scans. Some lifetime measurements were made with a pulsed alexandrite laser with about 5 mJ pulse energy and a pulse length of 10 ns.

The near-infrared absorption spectrum was measured by detection of monoanions produced by electron autodetachment after absorption of a photon from a laser pulse. The monoanions were detected with a channeltron placed close to the beam after a 10° deflection (Fig. 1). The laser was fired when the bunch of stored ions was about 1.5 m in front of the detector after a variable number of ion revolutions in the ring.

III. LIFETIMES

The stored dianions are unstable, and their decay by electron detachment was monitored by detection of monoanions in the channeltron.[15] After photon absorption the yield is strongly enhanced, and the time dependence of the enhancement is shown in Fig. 2 for three wavelengths. The first point of the time spectra corresponds to detachment within the first
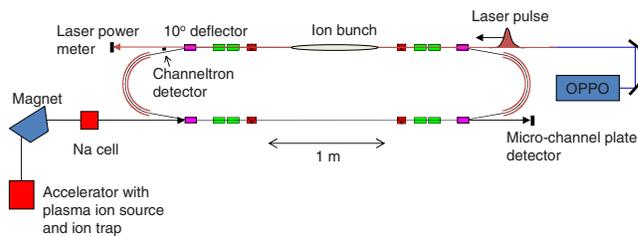

FIG. 1. Sketch of the electrostatic storage ring ELISA.

~20 μs, and the following points show the weaker enhancement after one or more revolutions of the ions in the ring. The points fall on straight lines in the semilog plot, consistent with exponential decay with the lifetimes indicated in the figure caption, except for the first point, which is too high by nearly an order of magnitude.

Internal conversion of electronic to vibrational excitation is known to take place on a subnanosecond time scale,[21,22] so the electron detachment observed after one or more revolutions of the beam must be due to a statistical process, i.e., vibrationally assisted electron tunneling. According to our modeling of the decay (see Fig. 7 in Ref. 15), the spectrum of microcanonical temperatures in the ensemble of ions ranges from below 100 to about 300 K, with an average temperature of about 200 K, for a trap temperature of 100 K and after storage for 10–16 ms in the ring. The spectrum after photon absorption and internal conversion is shifted to higher temperatures, with average values of about 490, 480, and 450 K for 735, 785, and 935 nm, and as demonstrated by the data in Fig. 2, the distributions in microcanonical temperature (or energy) are sufficiently narrow to give exponential decay. (When the variation in the rate constant over the energy distribution is large, the decay function is closer to a $1/t$ dependence, and the ions decaying at time t have a rate constant of $\sim 1/t$.)[23]

The high decay rate at very short times seen in Fig. 2 indicates that there is a competing process with very short lifetime, which we interpret as direct tunneling of the excited electron into the continuum (see also Ref. 24). With an estimated detection efficiency that is a factor of three higher for prompt decay than for delayed statistical decay, the probability for prompt decay is found to be about 0.4 with no significant dependence on photon energy. Note that the lifetime for direct tunneling is expected not to vary much with photon energy since the excited electronic state is the same at all photon energies.

Thus the lifetimes for direct tunneling from the excited state and for internal conversion of electronic to vibrational energy are found to be very similar. This is consistent with simple estimates of the lifetimes. For the monoanion C_{60}^-, the lifetime of an excited t_{1g} state has been measured to be 2.2 ps.[22] It may be expected to be somewhat shorter for the dianion partly because the excitation energy is about 10% higher and partly because the coupling to H_g vibrations is stronger than in the monoanion.[22] The excited state energy of about 1.5 eV is close to the maximum of the Coulomb barrier, about 1.7 eV,[15,25] so the decay rate is not much reduced by the barrier penetration. The attempt frequency used in the modeling was $\nu = 3 \times 10^{13}$ s^{-1}, and with an estimated
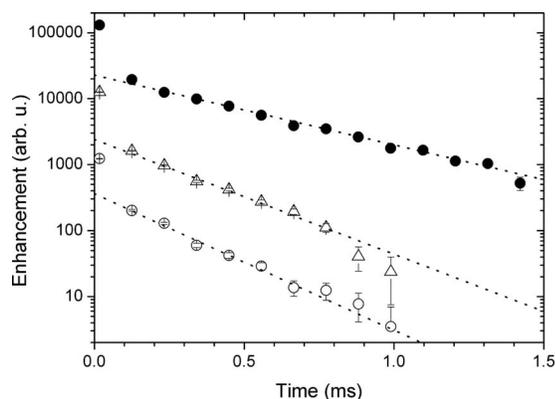
FIG. 2. Decay of stored C$_{60}^{2-}$ ions after absorption of a photon. The lower two time spectra are for photons from the alexandrite laser with (○) 735 nm and (△) 785 nm wavelengths absorbed at 15.5 ms after ion injection, and the upper spectrum (●) is for 935 nm photons from the OPO laser absorbed at 10.8 ms after injection. For all spectra the trap was cooled to a temperature below 100 K. The separation of the points is the revolution time in the ring. The dotted lines are fitted exponential decays with lifetimes of 0.21 ms (735 nm), 0.25 ms (785 nm), and 0.41 ms (935 nm).

penetration probability of 0.2 one obtains a lifetime of order 0.2 ps. The uncertainty on this estimate is rather large, but the lifetimes for the two competing processes are clearly expected to be of the same order of magnitude.

In the modeling in Ref. 15 of the decay of the C$_{60}^{2-}$ ions in the storage ring, the internal energy of the ions decaying at the shortest times was estimated on the basis of lifetime measurements in preliminary laser experiments. However, at the time we did not realize that there is a contribution from direct tunneling to the decay after photon absorption, and therefore the rate constant for statistical decay after internal conversion was overestimated by an order of magnitude. The implication is that the tail of the internal energy spectrum toward higher energies is even more pronounced than assumed in the modeling. The tail is produced partly by collisions with residual gas molecules just after extraction from the ion trap partly by electron transfer to excited states in the Na cell. This modification has no influence on the modeling of the decay of the ion ensemble at later times.

IV. ABSORPTION SPECTRA

From the variation with wavelength of the enhancement of the C$_{60}^{-}$ signal normalized to the number of photons, the absorption spectrum was obtained. In Fig. 3 results are compared with absorption spectra for dianions in solution. All spectra have a main absorption band near 10 600 cm^{-1}, which is better resolved at the lower temperatures. The peak is at 10 723 cm^{-1} in the gas-phase spectra with 3 cm^{-1} subtracted for the Doppler shift. The general shape of our spectra is similar to the spectrum for C$_{60}^{2-}$ in benzonitrile at room temperature apart from broadening and a small redshift in the solution. Very similar spectra were also observed in Refs. 28 and 13, where the singlet character of the ground state was established from measurements of electron spin resonance. As discussed below, the JT interaction is quite different in the triplet states, so the close similarity of the spectra indicates that the ground state is singlet also in the gas phase.
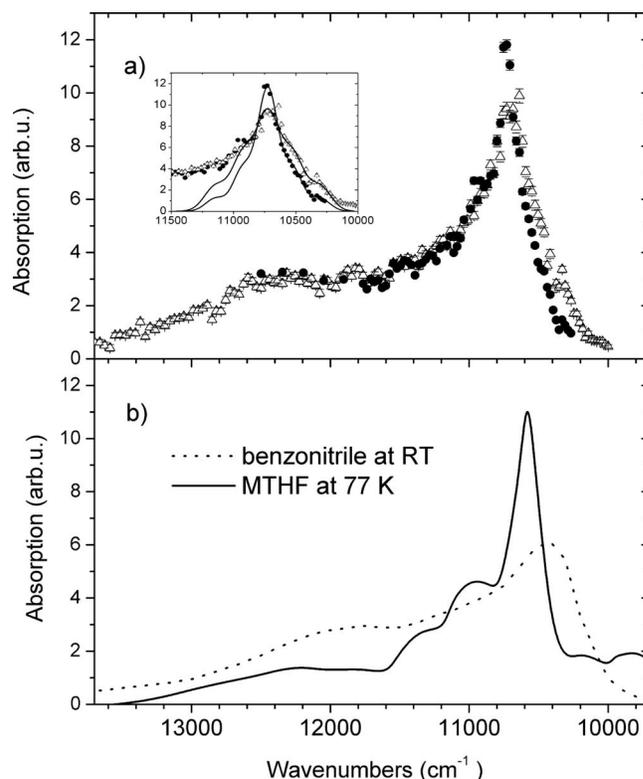

FIG. 3. (a) Absorption spectra for $T_{trap} \simeq 300$ K (△) and $T_{trap} \lesssim 100$ K (●) with delays between ion injection and laser pulse set to 10.8 and 32 ms, respectively. The inset shows the peak region with fits discussed in the text. (b) Absorption spectra for C$_{60}^{2-}$ ions in MTHF at 77 K (Ref. 26) and in benzonitrile at room temperature (Ref. 27).

The simplest interpretation of the spectra is a transition from the t_{1u} lowest unoccupied molecular orbital (LUMO) level of C$_{60}$ to the t_{1g} LUMO+1 level, both triply degenerate. The notation refers to subgroups of the icosahedral point group, but we may think of p-type orbitals with odd and even symmetries, respectively. For the interpretation it is very helpful to compare with the gas-phase absorption spectrum for the monoanion shown in Fig. 4. As for the dianion, there is a main absorption band, redshifted in solution. There are sidebands from vibrational excitation because the equilibrium deformation is different in the initial and final states, and similar bands should be contained in the broad tail toward higher energies in the spectrum for the dianion. Even stronger sidebands are observed in photodetachment from monoanions with a UV laser, where there is no distortion in the final (neutral) state of the molecule.[31,32]

A. JT coupling

To interpret the C$_{60}^{2-}$ spectra in more detail we first consider the JT coupling in the initial $(t_{1u})^2$ electronic configuration.[7,8] The main JT interaction is with the eight H_g vibrations illustrated in Fig. 5. (We ignore the interaction with two A_g vibrations, which do not contribute to the JT splitting.) For triplet states, the JT problem is identical to the one for a single electron, but in the singlet ground state, with two electrons in the same orbital, the JT coupling is twice as strong as in the monoanion. As discussed above, we may assume that the electronic state is singlet. The orbital trans-
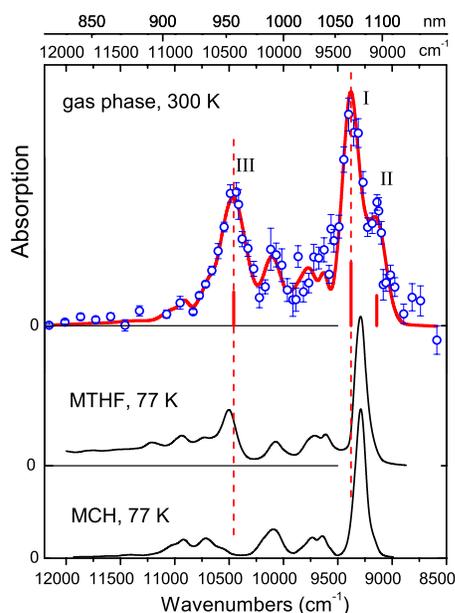
FIG. 4. Absorption spectra for C_{60}^- in the gas phase at $\simeq 300$ K (top) (Ref. 21), in a MTHF matrix at 77 K (middle) (Ref. 29), and in methylcyclohexane at 77 K (bottom) (Ref. 30).

forms as a vector under rotations in three dimensions; in the adiabatic approximation, the electron orbitals and the deformation are strongly coupled and rotate together, and the most important low-energy excitations correspond to such so-called pseudorotations of the molecule.

For linear JT coupling, the energy eigenstates have a well-defined pseudo-angular-momentum $L\hbar$ and symmetry requires L to be even. The pseudorotational energy is given by

$$E_{\text{rot}}(L) = \frac{L(L+1)}{24k^2}, \qquad (1)$$

in units of a weighted average of the energies of the H_g vibrations involved in the JT distortion. The effective moment of inertia is proportional to the square of the deformation, and since the equilibrium value of the deformation in the singlet ground state is twice as large as for the monoanion, the denominator in Eq. (1) is four times as large as in the corresponding formula for C_{60}^- [Eq. 2 in Ref. 21]. From an analysis of a photoelectron spectrum for C_{60}^-,[31] the average vibrational energy was estimated to be $\hbar\omega_0 \simeq 600$ cm^{-1}, and the value of $k^2 \simeq 2.4$ was obtained for the square of the JT-coupling parameter. As in Ref. 21 we shall use the value of $k^2 \sim 2$ in estimates of JT energies, and the two lowest excited levels are then at 75 cm^{-1} ($L=2$) and 250 cm^{-1} ($L=4$).

In the excited electronic state one electron is in a t_{1g} orbital, for which the JT coupling constant is similar in magnitude but has the opposite sign. The minimum of the total JT energy is therefore obtained for a so-called bimodal deformation, which is the same as that of the ground state of C_{60}^{3-} discussed in Refs. 7 and 8. The Hamiltonian is that of a symmetric top, and the energy depends on the total pseudo-angular-momentum $L\hbar$ and its projection $K\hbar$ on the symmetry axis,
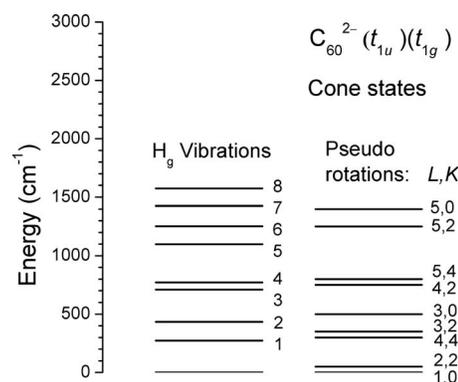

FIG. 5. To the left are indicated the energies of the eight H_g vibrations in C_{60} and to the right are energies from Eq. (2) of JT states of C_{60}^{2-} in the excited electronic state $(t_{1u})(t_{1g})$ relative to the energy of the lowest state, $(L,K)=(1,0)$.

$$E_{\text{rot}}(L,K) = \frac{1}{6k^2}\left(L(L+1) - \frac{3}{4}K^2\right), \qquad (2)$$

with the units in Eq. (1). Symmetry requires K to be even and $K=0$ is only allowed for odd L. Energy levels are shown in Fig. 5. We note that the rotational constant in Eq. (2) is the same as for pseudorotations of the monoanion.[21]

B. Interpretation of spectra

We now turn to the interpretation of the spectra in Fig. 3(a) and first consider the region close to the main peak, shown in detail in the inset. The region of the peak and the slope toward lower energies are fitted with three Gaussians, a main band at 10 723 cm^{-1} and weaker bands at 10 523 and 10 303 cm^{-1} with standard deviations of $\sigma=80$ cm^{-1} and $\sigma=90$ cm^{-1} for the two spectra. To aid the discussion, we have added symmetrically two Gaussians at higher energies. The two spectra in Fig. 3(a) are recorded for ions with different distributions in internal energy. From modeling as described in Ref. 15 the average microcanonical temperatures are estimated to be of the order of 200 and 300 K. The peak at 10 523 cm^{-1} cannot be a sideband with destruction of a vibrational excitation since there should then be a symmetrically placed sideband for vibrational excitation with much higher intensity. The natural interpretation is that this peak is a transition from an excited pseudorotational state to the same final state, $(L,K)=(1,0)$. Relative to the main peak, the heights of the peaks displaced by -200 cm^{-1} are 34% and 58% at 200 and 300 K, respectively, and the relative strength in the two spectra is consistent with this interpretation. Probably the peak at 10 303 cm^{-1} should be interpreted in a similar way.

According to Eq. (1) the excited state at 200 cm^{-1} could be $L=4$. A dipole transition to $(L,K)=(1,0)$ is not allowed from this level ($|\Delta L| \leq 1$), but there are significant nonlinear effects giving a warping of the JT-potential-energy surface and consequent mixing of states with different L.[7,8] The nonlinearity is not very strong for the monoanion,[8,31] but it must be more pronounced for the singlet ground state of the dianion because the JT coupling is twice as strong. The symmetries of the eigenstates should then be specified under the

icosahedral group, e.g., A_g, H_g, $G_g \oplus H_g$, and $A_g \oplus T_{1g} \oplus G_g \oplus H_g$ instead of $L=0$, $L=2$, $L=4$, and $L=6$, and the selection rules are modified.

As mentioned above, the continuum for photon energies just above the main peak should contain sidebands corresponding to excitations of H_g vibrations that appear because the JT deformation is different in the initial and final electronic states. There may also be transitions to excited pseudorotational states. Note that the two level spectra in Fig. 5 are of a very different nature. The energy levels of H_g vibrations to the left are the spacings in independent harmonic oscillators, while the spectrum to the right is the low-energy part of the complete spectrum of excitations of the three vibrational degrees of freedom converted to pseudorotations.

The vibrations are excited by shake up in the transition, and since the equilibrium deformation in the final electronic state is a compromise between the optimum deformations for the two electrons with opposite signs of JT interaction, the deformation change is not very different from that experienced by C$_{60}^-$ in the corresponding transition. The sidebands seen in the well resolved spectrum at the bottom of Fig. 4 can all be accounted for as single excitations of the H_g vibrations illustrated in Fig. 5. As seen in Fig. 5, it is therefore very unlikely that such bands can account for the absorption at the highest energies. There may be multiple excitations corresponding to overtones of the vibrational frequencies, but they should be weaker.[32]

C. Transitions to cone states

A possible explanation of the strong absorption at high energies is transition to so-called cone states, which are JT states with the opposite sign of the deformation amplitude and positive JT energy.[33–35] In the JT ground state the magnitude of the deformation amplitude q is determined by a balance between the JT force driving the deformation and the harmonic restoring force, but for cone states with the opposite sign of q these forces act together to reduce the magnitude of q. The deformation is instead stabilized by the centrifugal force associated with pseudorotations.

Let us see whether the observation of transitions to final states 2000–3000 cm^{-1} above the lowest JT level for the excited electronic state is consistent with this explanation. The lowest JT energy is of the order of $-(3/2)k^2\hbar\omega_0 \simeq -1800$ cm^{-1}, and since the JT energy of cone states should be positive and there should also be a pseudorotational energy to stabilize the states, the total energies should be higher by at least ~ 3000 cm^{-1}. However, the energy could be somewhat lower if the reversed deformation is stable only for the lower-frequency H_g vibrations. According to the analysis in Ref. 34, the reversed deformation can be stabilized by pseudorotation only if the frequency of rotation is higher than the vibrational frequency.

To estimate the rotation frequency, we use the classical relation $L\hbar = I\omega_r$, where I is the moment of inertia and ω_r is the rotation frequency. The energy is $L(L+1)\hbar^2/2I$ and from a comparison with Eq. (2) with $K=0$, we obtain $I = 3k^2\hbar/\omega_0$. Inserting this into the above relation between L and ω_r we obtain $\omega_r/\omega_0 = L/3k^2$. For a vibration with fre-

quency ω the stability requirement $\omega < \omega_r$ then becomes $\omega < (L/3k^2)\omega_0$. With $k^2 \sim 2$, the factor on ω_0 is less than unity except for very large L, and the relation is only fulfilled for the lowest vibrational frequencies in Fig. 5.

However, when we consider the stability of cone states, we should think of the energy as a pseudo-angular-momentum barrier. The moment of inertia is proportional to the square of the deformation amplitude q, and the pseudorotational energy proportional to q^{-2} prevents collapse, $q \to 0$. It therefore seems appropriate to evaluate the stability criterion at a somewhat smaller deformation, say, about half of the equilibrium deformation corresponding to Eq. (2). We should then insert the value of $k^2 \simeq 1/2$ into the stability criterion above, and for $L=3$ we obtain $\omega < 2\omega_0$. This is well fulfilled for the lower-energy vibrations in Fig. 5 but excludes the upper three energies.

From these estimates it appears that transitions to final states with a reversed deformation for only some of the H_g vibrations might be an explanation for the broad high-energy band in the absorption spectra. Admittedly, this assignment is somewhat speculative, and we have not found any theoretical work on such states, except for a remark in Ref. 34. However, the assignment is supported by a strong qualitative argument: the absorption spectrum for the dianion is nearly twice as broad as for the monoanion, while vibrational sidebands and pseudorotational excitations in the final electronic state should be very similar for the two ions. The JT energy is three times larger in the final state for the dianion, but it seems that the only way this energy can come into play is through the Slonczewski mechanism of excitation to states on a higher JT-potential-energy surface.[34]

With the new information on absorption in C$_{60}^{2-}$ we may take a fresh look at the interpretation of the absorption spectra for the monoanion in Fig. 4. The band III in the top spectrum was in Ref. 21, interpreted as a transition from an excited JT state (T_{2u} with a t_{1u} electronic orbital) to a pseudorotational final state with $L=4$ and with a t_{1g} electronic orbital, but the calculated transition energy was about 25% too low. An alternative explanation might be a transition to a cone state. Band III is 1315 cm^{-1} higher in energy than band II, and this separation is about right. Compared with the estimate above for cone states of C$_{60}^{2-}$, the JT potential energy is lower by a factor of three, while the pseudorotational energies are the same.

The special interpretation of the high-energy part of the absorption spectra for the dianion in Figs. 3(a) and 6 is supported by a comparison with the absorption spectrum in Fig. 3(b) for C$_{60}^{2-}$ ions at 77 K in frozen 2-methyltetrahydrofuran (MTHF). It was obtained from the trace h in Fig. 1 in Ref. 26 after subtraction of a linear background. (At higher irradiation doses there are indications of a small contribution from absorption in trianions.)[36] Apart from the small redshift, the low-energy part of the spectrum is not very different from the gas-phase spectra. The signal below the peak at 10 600 cm^{-1} is due to absorption by monoanions, which extends up to about 11 000 cm^{-1} (Fig. 4, bottom) and explains the steep decrease just above 11 000 cm^{-1}. However, there is also a marked drop in absorption around 11 500 cm^{-1}, and the relative strength of the absorption between 11 600 and
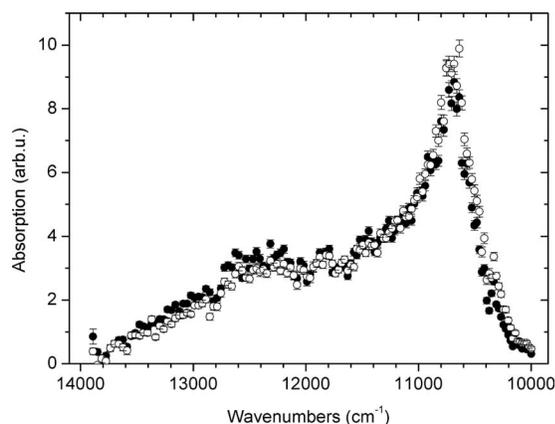
FIG. 6. Photoabsorption by stored C_{60}^{2-} ions at 10.8 ms after ion injection. The trap temperatures were $T_{\text{trap}} \simeq 300$ K (open circles) and $T_{\text{trap}} \lesssim 100$ K (full circles).

13 600 cm^{-1} is lower by about a factor of two than in benzonitrile at room temperature and in the gas-phase spectra.

The most likely explanation for this difference is the temperature difference. For free ions we see no decrease in the high-energy absorption with decreasing temperature, as indicated in Fig. 3(a) and illustrated in Fig. 6 by a comparison of two complete scans with the same laser delay time but different temperatures of the ion trap. However, if the energy of the lowest five-fold degenerate H_g level relative to the A_g ground state is close to the estimated 75 cm^{-1}, the populations of the two levels are about equal at 77 K. For the gas-phase spectra in Figs. 3 and 6, the average (microcanonical) temperature of the ions is much higher, $T \sim 200-300$ K, and the population of A_g is only $\simeq 17\%$. A very low strength of optical transitions from the JT ground state to cone states could therefore explain the observed reduction in the high-energy part of the MTHF spectrum in Fig. 3(b). This is not unreasonable since, as discussed above, the stabilization of cone states requires a significant pseudo-angular-momentum, and dipole transitions from the A_g ground state may be forbidden.

This explanation of the temperature dependence of the high-energy absorption band for C_{60}^{2-} is analogous to the interpretation in Ref. 21 of the temperature dependence of band III in the top spectrum for the monoanion in Fig. 4. The lowest pseudo-rotational excitation in the electronic ground state is for this case so high that the transition from this excited state to the lowest JT level for the final electronic state is resolved (band II). Neither band II nor band III are observed at 77 K, and it was concluded that band III also corresponds to transitions from the excited state.

Note that the small peak near the position of band III for absorption in an MTHF matrix at 77 K (middle spectrum in Fig. 4) is a contamination from absorption in dianions, and the discussion of this peak in Ref. 21 and in earlier work[8,29] was based on an incorrect assignment. The middle spectrum in Fig. 4 was obtained with the same technique as applied in Ref. 26, where absorbance spectra were recorded for a sequence of γ-irradiation levels with increasing concentration of free electrons. The series of traces in Fig. 1 in Ref. 26 reflects the initial formation of C_{60}^- ions and gradual conver-

sion to dianions. Trace *d* in this series is very similar to the middle spectrum in Fig. 4, and it is clear that the peak near 10 600 cm^{-1} belongs to the dianion spectrum and not to that of the monoanion. At higher irradiation levels, this peak evolves into the main absorption peak in trace *h*, shown as the full-drawn spectrum in Fig. 3(b).

It appears that we have obtained a consistent picture of the near-infrared absorption spectra for the monoanions and dianions of C_{60}, but support from detailed theoretical calculations is needed. In this respect, a recent study of the electronic level density in a C_{60}^- molecule is very interesting.[37] The current through a single C_{60} molecule was measured by scanning-tunneling microscopy (STM) as a function of bias voltage, and for negative bias of the STM tip, the derivative of the current with respect to voltage is proportional to the density of unoccupied levels in the molecule. The main features of the measured spectrum are a sharp main peak and a broad sideband at about 1850 cm^{-1} higher energy.

The measurements are compared with density-functional calculations including JT coupling. The injection of an electron into the C_{60} molecule is the inverse of electron detachment, for example, photoemission.[32] As in the photoelectron spectrum analyzed in Ref. 32 there are sidebands from excitation of vibrations due to a change in the equilibrium deformation now in C_{60}^- and slightly shifted in energy due to the JT interaction. The calculations also reproduce the broad sideband at about 1850 cm^{-1}, and a comparison to calculations with JT coupling to the different vibrations separately shows that this sideband results from the combined interaction with all the vibrations. The origin of the band is not discussed in detail in Ref. 37, but it is tempting to assign it to a combination of two narrow sidebands corresponding to the highest vibrational frequencies and cone states with positive JT energy from the interaction with the lower-frequency vibrations.

Qualitatively, this interpretation is consistent with our new interpretation of band III in Fig. 4. The separation of 1315 cm^{-1} between bands II and III is smaller than the separation of 1850 cm^{-1} between the main level density peaks for the LUMO level, but this might be due to the JT interaction in the LUMO+1 level being weaker by $\sim 15\%$. It should also be noted that in earlier absorption measurements for C_{60}^- in solution, the high-energy band was observed at somewhat higher energy.[38] We plan to repeat the gas-phase experiment for C_{60}^- with the new, more stable ion source and with a more powerful laser to check the positions of the bands and determine the temperature dependence of their strength.

V. SUMMARY AND CONCLUSIONS

In summary, we have reported near-infrared absorption spectra of C_{60}^{2-} ions in the gas phase. The absorption leads to electron loss and both direct electron tunneling into the continuum and statistical autodetachment after internal conversion are observed. Since the excited electronic state is close to the maximum (~ 1.7 eV) of the Coulomb barrier calculated in Ref. 15, this is evidence against the suggestion in Ref. 6 of much lower Coulomb barriers for fullerene dianions and is consistent with a recent determination by photo-

emission of a 1.6 eV Coulomb barrier for C$_{70}^{2-}$ (Ref. 39) and slightly lower values for C$_{76}^{2-}$, C$_{78}^{2-}$, and C$_{84}^{2-}$.[40]

The absorption spectra reveal the strong JT interaction in the dianions of C$_{60}$, and the electronic ground state is determined to be singlet. Transitions from both the JT ground state and excited pseudorotational states have been observed. There is evidence for interpretation of a broad high-energy band as transitions to states with positive JT energy stabilized by pseudorotations (cone states), and we suggest a similar assignment for a high-energy absorption band in the monoanion.

ACKNOWLEDGMENTS

[1] S. E. Erwin and W. E. Pickett, Science **254**, 842 (1991).

[2] M. Capone, M. Fabrizio, C. Castellani, and E. Tosatti, Science **296**, 2364 (2002).

[3] A. V. Danilov, P. Hedegård, D. S. Golubev, T. Bjørnholm, and S. E. Kubatkin, Nano Lett. **8**, 2393 (2008).

[4] C. A. Martin, D. Ding, J. Kryger Sørensen, T. Bjørnholm, J. M. van Ruitenbeek, and H. S. J. van der Zant, J. Am. Chem. Soc. **130**, 13198 (2008).

[5] M. K. Scheller, R. N. Compton, and L. S. Cederbaum, Science **270**, 1160 (1995).

[6] O. T. Ehrler, F. Furche, J. M. Weber, and M. M. Kappes, J. Chem. Phys. **122**, 094321 (2005).

[7] M. C. M. O'Brien, Phys. Rev. B **53**, 3775 (1996).

[8] C. C. Chancey and M. C. M. O'Brien, *The Jahn–Teller Effect in* C$_{60}$ *and Other Icosahedral Complexes* (Princeton University Press, Princeton, NJ, 1997).

[9] A. V. Nikolaev and K. H. Michel, J. Chem. Phys. **117**, 4761 (2002).

[10] J. E. Han, E. Koch, and O. Gunnarsson, Phys. Rev. Lett. **84**, 1276 (2000).

[11] O. Gunnarsson, J. E. Han, E. Koch, and V. H. Crespi, Struct. Bond. (Berlin) **114**, 71 (2005).

[12] C. A. Reed and R. D. Bolskar, Chem. Rev. (Washington, D.C.) **100**, 1075 (2000).

[13] P. R. Trulove, R. T. Carlin, G. R. Eaton, and S. S. Eaton, J. Am. Chem. Soc. **117**, 6265 (1995).

[14] B. Liu, P. Hvelplund, S. B. Nielsen, and S. Tomita, Phys. Rev. Lett. **92**, 168301 (2004).

[15] S. Tomita, J. U. Andersen, H. Cederquist, B. Concina, O. Echt, J. S. Forster, K. Hansen, B. A. Huber, P. Hvelplund, J. Jensen, B. Liu, B. Manil, L. Maunoury, S. B. Nielsen, J. Rangama, H. T. Schmidt, and H. Zettergren, J. Chem. Phys. **124**, 024310 (2006).

[16] S. P. Møller, Nucl. Instrum. Methods Phys. Res. A **394**, 281 (1997).

[17] J. U. Andersen, P. Hvelplund, S. B. Nielsen, S. Tomita, H. Wahlgreen, S. P. Møller, U. V. Pedersen, J. S. Forster, and T. J. D. Jørgensen, Rev. Sci. Instrum. **73**, 1284 (2002).

[18] K. O. Nielsen, Nucl. Instrum. Methods **1**, 289 (1957).

[19] D. H. Yu, L. H. Andersen, C. Brink, and P. Hvelplund, Mol. Mater. **4**, 237 (1994).

[20] H. Zettergren, M. Alcami, and F. Martin, Phys. Rev. A **76**, 043205 (2007).

[21] S. Tomita, J. U. Andersen, E. Bonderup, P. Hvelplund, B. Liu, S. B. Nielsen, U. V. Pedersen, J. Rangama, K. Hansen, and O. Echt, Phys. Rev. Lett. **94**, 053002 (2005).

[22] O. T. Ehrler, J. P. Yang, C. Hättig, A.-N. Unterreiner, H. Hippler, and M. M. Kappes, J. Chem. Phys. **125**, 074312 (2006).

[23] K. Hansen, J. U. Andersen, P. Hvelplund, S. P. Møller, U. V. Pedersen, and V. V. Petrunin, Phys. Rev. Lett. **87**, 123401 (2001).

[24] O. T. Ehrler, J.-P. Yang, A. B. Sugiharto, A. N. Unterreiner, and M. M. Kappes, J. Chem. Phys. **127**, 184301 (2007).

[25] There is an error in the plot of the barrier in Fig. 6 in Ref. 15. The division by two of the second term in Eq. (1) was omitted.

[26] H. Hase, Y. Kitajima, Y. Miyamoto, Y. Miyataki, Y. Tajima, and M. Hoshino, Chem. Phys. Lett. **326**, 186 (2000).

[27] D. V. Konarev, N. V. Drishko, V. N. Semkin, and A. Graja, Synth. Met. **103**, 2384 (1999).

[28] D. R. Lawson, D. L. Feldheim, C. A. Foss, P. K. Dorhout, C. M. Elliott, C. R. Martin, and B. Parkinson, J. Electrochem. Soc. **139**, L68 (1992).

[29] H. Kondo, T. Momose, and T. Shida, Chem. Phys. Lett. **237**, 111 (1995).

[30] J. Fulara, M. Jakobi, and J. P. Maier, Chem. Phys. Lett. **211**, 227 (1993).

[31] O. Gunnarsson, H. Handschuh, P. S. Bechthold, B. Kessler, G. Ganteför, and W. Eberhardt, Phys. Rev. Lett. **74**, 1875 (1995).

[32] X.-B. Wang, H.-K. Woo, and L.-S. Wang, J. Chem. Phys. **123**, 051106 (2005).

[33] H. C. Longuet–Higgins, O. Öpik, M. H. L. Pryce, and R. A. Sack, Proc. R. Soc. London **A244**, 1 (1958).

[34] J. C. Slonczewski, Phys. Rev. **131**, 1596 (1963).

[35] T. Sato, L. F. Chibotaru, and A. Ceulemans, J. Chem. Phys. **122**, 054104 (2005).

[36] G. A. Heath, J. E. McGrady, and R. L. Martin, J. Chem. Soc., Chem. Commun. **17**, 1272 (1992).

[37] T. Frederiksen, K. J. Franke, A. Arnau, G. Schulze, J. I. Pascual, and N. Lorente, Phys. Rev. B **78**, 233401 (2008).

[38] R. D. Bolskar, S. H. Gallagher, R. S. Armstrong, P. A. Lay, and C. A. Reed, Chem. Phys. Lett. **247**, 57 (1995).

[39] X.-B. Wang, H.-K. Woo, X. Huang, M. M. Kappes, and L.-S. Wang, Phys. Rev. Lett. **96**, 143002 (2006).

[40] X.-B. Wang, H.-K. Woo, J. Yang, M. M. Kappes, and L.-S. Wang, J. Phys. Chem. C **111**, 17684 (2007).